DOI: 10.24352/UB.OVGU-2018-012 TECHNISCHE MECHANIK, 38, 1, (2018), 126 – 134
submitted: July 24, 2017

Discrete-Continuum Transition: A Discussion of the Continuum Limit

K. Schulz, S. Schmitt

In recent years, the striving towards a proper understanding of plastic deformation on different scales led to a substantial progress in the development of advanced dislocation based material models. In this paper the limits of a continuum representation of dislocation dynamics in the discrete to continuous transition regime are discussed. Using 2d discrete dislocation dynamic simulations, a systematic investigation of ensemble averages of a bounded structure is presented considering a varying number of dislocations. Based on the results, the question, how we can evaluate the conditions under which a discrete system behaves similarly to a homogenized continuum system, is discussed.

1 Introduction

Several dislocation based continuum models have been introduced in the last decades, e.g. (Acharya, 2001; Sedláček et al., 2003; Groma, 1997; Groma et al., 2003; El-Azab, 2000; Hochrainer et al., 2014). Applying different approaches for the kinematic assumptions, all models depend on an adequate homogenization of internal stress fields induced by the dislocation microstructure. Different stress-based formulations have been introduced considering e.g. repellent and attractive stresses (Groma et al., 2003; Schulz et al., 2014; Schmitt et al., 2015; Hochrainer, 2016), dipole formation and dissolution (Reuber et al. (2014); Dickel et al. (2014b); Schulz et al. (2017)), or interactions between different slip systems (Franciosi and Zaoui, 1982; Devincre et al., 2008; Devincre and Gatti, 2015; Zhu et al., 2016). However, the limits of the different continuum formulations in the discrete-continuous transition regime have not been investigated yet and are therefore almost unknown.

The results of dislocation based continuum models are often validated by the comparison with discrete dislocation dynamics (DDD) data. In the discrete models, see e.g. (Kubin and Canova, 1992; Fivel et al., 1997; Weygand et al., 2002), each dislocation line is resolved including the corresponding stress field. Thus, the stress interaction in the dislocation microstructure is an outcome of a simulation without any homogenization or phenomenological parameter. In general, discrete simulations are - in the considered regimes - highly dependent on the initial dislocation configuration. Therefore, a common procedure is to average the results of several statistically equivalent simulations by ensemble averaging in order to get robust mean values.

In contrast, a continuum model aims to represent a regime characterized by a 'continuum limit', in which a single computation is sufficient to comprise all significant details of a structure. This is the case, if

(I) the considered system of discrete simulations show the same results as continuum theories (Cleveringa et al. (1997))

(II) the simulations show a weak dependency on the initial dislocation distribution (Zaiser (2015)).

Without further analyses, it is often assumed that these conditions are fulfilled if a system contains a sufficiently high number of dislocations. In addition, a consideration of stress correlation in dislocation systems is mostly given for periodic structures, e.g. (Groma et al., 2003; Zaiser, 2015), neglecting any internal boundaries or heterogeneities. In this paper, we analyze 2d DDD simulations by a systematic investigation of ensemble averages. Using pair correlations, we study a bounded structure considering a varying number of dislocations and compare DDD data with results of two homogenized continuum formulations. We show, that the determination of the continuum limit is not a trivial task and highly dependent on the structure of the system, e.g. the influence of boundaries on the one hand and the particular stress homogenization of a dislocation based continuum model on the other hand.

2 Continuum Framework and DDD Method

We use a 2d model of discrete dislocation dynamics which is almost identical to that described in Groma et al. (2003). We consider a single slip system of parallel edge dislocations. The dislocations with the position $\mathbf{x_i}(x_i, z_i)$ and the orientation $s = \pm 1$ are free to move in x-direction. Impenetrable boundaries in x-direction are defined by setting the increment $\Delta x_i = 0$ if a dislocation face the boundary with a velocity pointing out of the bounded domain. The constitutive law is defined by the overdamped dislocation motion as

$$v_i = bB^{-1}s_i\tau = bB^{-1}s_i(\tau_{ext} + \tau_{sc}) \tag{1}$$

with the magnitude of the Burger's vector b and the drag coefficient B. The resolved shear stress τ acting on a dislocation is composed of the externally applied stress τ_{ext} and the self-consistent stress field τ_{sc} representing internal stress interaction among the dislocations. Considering the stress field of a single edge dislocation, see Hirth and Lothe (1982), τ_{sc} is given as

$$\tau_{sc} = \sum_{i\neq j}^{N} s_j \frac{\mu b}{2\pi(1-\nu)} \frac{(x_i - x_j)((x_i - x_j)^2 - (z_i - z_j)^2)}{((x_i - x_j)^2 + (z_i - z_j)^2)^2} \tag{2}$$

with the shear modulus μ and the Poisson's ratio ν. Due to the stress interaction, a bounded system of dislocations randomly placed over the area will relax towards a converged state.
In order to derive a continuous description out of discrete dislocation dynamics simulation, we consider ensemble averages over a number of statistically equivalent microstructures. We assume, that the average of the number of realizations m converges for $m \to \infty$. For a discrete simulation with n dislocations $\{s_i, \mathbf{x_i}\}_{i=1,\dots,n}$, the 1-particle distribution function can be written as

$$\rho_1^d(s, \mathbf{x}) = \left\langle \sum_{i=1}^{n} \delta_{ss_i}\delta(\mathbf{x} - \mathbf{x_i}) \right\rangle. \tag{3}$$

The 2-particle distribution function considering dislocations of the signs $s, s' \in \{+, -\}$ is given as

$$\rho_2^d(s, s', \mathbf{x}, \mathbf{x}') = \left\langle \sum_{i=1}^{n}\sum_{j\neq i}^{n} \delta_{ss_i}\delta_{s's_j}\delta(\mathbf{x} - \mathbf{x_i})\delta(\mathbf{x}' - \mathbf{x_j}) \right\rangle. \tag{4}$$

Here, δ denotes the Dirac functional and $\langle\cdot\rangle$ denotes the integration over the given averaging volume around $\mathbf{x}$. Considering the k-particle density functions ρ_k^d of m statistically equivalent simulation, the ensemble average can then be defined as

$$\rho_k(s_1, ..., s_k, \mathbf{x}_1, ..., \mathbf{x}_k) = \frac{1}{m}\sum_{i=1}^{m} \rho_k^d(s_1, ..., s_k, \mathbf{x}_1, ..., \mathbf{x}_k). \tag{5}$$

The evolution equations (1) can equivalently be formulated for the N-particle distribution function (for N dislocations) and a hierarchy of evolution equations can be deduced for any lower order particle distribution function. The hierarchy of particle density functions can be closed at second order according to Groma (1997) and Zaiser et al. (2001) by the introduction of the dislocation-dislocation or pair correlation function $d_{ss'}$. Thus, the 2-particle distribution function can be defined by

$$\rho_2(s, s', \mathbf{x}, \mathbf{x}') = \rho_1(s, \mathbf{x})\rho_1(s', \mathbf{x}')(1 + d_{ss'}(\mathbf{x}, \mathbf{x}')). \tag{6}$$

Since the averaging of a homogeneous distribution of dislocations on a bounded domain does not lead to a vanishing pair correlation function, the influence of the bounded domain is characterized analytically by a relative 1-particle density function. The relative 1-particle density function is given for homogeneous dislocation distributions on a bounded domain as

$$\rho_1^h(\mathbf{x}) = \frac{\rho_t \int \mathbf{I}_\Omega(\mathbf{x} - \mathbf{x}')d\mathbf{x}'}{\int_\Omega 1 d\mathbf{x}'} \qquad \text{with} \quad \mathbf{I}_\Omega = \begin{cases} 1 & \text{for } \mathbf{x} \in \Omega \\ 0 & \text{else.} \end{cases} \tag{7}$$

The relative correlation function, which is equivalent to a screened correlation function, see Ispanovity et al. (2008),

can then be written as

$$d_{ss'}(\mathbf{x}) = \begin{cases} \frac{\rho_2(s,s',\mathbf{x})}{\rho_1^h(\mathbf{0})\rho_1^h(\mathbf{x}')} - 1 & \text{for } 0 < x < L \text{ and } 0 < z < H \\ 0 & \text{else} \end{cases} . \tag{8}$$

For $\tau_{ext} = 0$, it holds $d_{++} = d_{--}$ and $d_{+-} = d_{-+}$.
In order to compare the results derived by discrete simulations with dislocation based continuum models, the discrete results have to be ensemble averaged. The continuum quantities of the geometrically necessary dislocation (GND) densities of positive dislocations κ_+ and negative dislocations κ_- as well as the total dislocation density ρ including also statistically stored dislocation (SSD) density can be derived by the ensemble average considering the same spacial resolution in the discrete and the continuum realization of the structure. Here, the discrimination of the density into GND and SSD density is dependent on the resolution. Thus, for an infinite fine resolution the transition to the discrete picture is given.
The considered 2d continuum model as proposed in Groma et al. (2003) or derived as 2d simplification from a 3D model according to Hochrainer et al. (2014) and Schulz et al. (2014) is defined by the evolution equations

$$\partial_t \rho = -\partial_x(\kappa v) \tag{9}$$
$$\partial_t \kappa = -\partial_x(\rho v). \tag{10}$$

The set of equations is closed by the assumption, that the velocity v of a given dislocation microstructure is known or determined by the dislocation microstructure. In analogy to the discrete formulation in equation (1), we assume, that the velocity can be defined dependent on the external and the internal stress contributions as $v = \tau_{ext} + \tau_{int}$ in the continuum approach. For the representation of the homogenized internal stress interactions contained in τ_{int}, we will compare the two different formulations

$$v_{\text{nfc}} = bB^{-1}(\tau_{\text{es}} + \tau_{\text{nfc}}) \tag{11}$$
$$v_{\text{b}} = bB^{-1}(\tau_{\text{es}} + \tau_{\text{b}}) \tag{12}$$

including the backstress τ_{b} with the free parameter D according to Groma et al. (2003) and the nearfield correction term τ_{nfc} according to Schmitt et al. (2015). The latter is based on the consideration of stress correlations in Dickel et al. (2014a) incorporating a constant c and the resolution h^* of the dislocation density. The terms are given as

$$\tau_{\text{nfc}} = -\frac{c\mu b}{(1-\nu)} \cdot \begin{cases} h^* \partial_x \kappa(x) & \text{if } N_{el}(x) \leq 1 \\ \rho(x)^{-1} \partial_x \kappa(x) & \text{else} \end{cases} , \qquad \tau_{\text{b}} = -D\mu b \cdot \rho(x)^{-1} \partial_x \kappa(x) . \tag{13}$$

If it holds $N_{el}(x) \leq 1$ for the number of dislocations inside an averaging element $N_{el}(x)$, the discrete near field correction is recovered up to a constant. If more than one dislocation is contained within the averaging volume, the formulation is identical to τ_{b}. τ_{es} denotes a numerical approximation of the self-consistent stress field τ_{sc} limited by the underlying resolution.

3 Bounded Slip Channel

We consider a bounded slip channel with the width L and the height H embedded into an infinite elastic medium, see Fig.1. A varying number of discrete positive edge dislocations is randomly distributed over the channel and free to move in x-direction. The boundaries at $x = 0$ and $x = L$ are impenetrable to dislocations, the external stress is given as $\tau_{ext} = 0$. Considering different numbers of dislocations homogeneously distributed over the system, we let the system relax. For a number of $n = 400$ dislocations, the results of the 1-particle density averaged over $m = 200$ discrete simulations is shown in Fig.2. Here, the 1-particle density according to equation (3) is symmetrized along the x- and z-axis and normalized with respect to the average total dislocation density ρ_t. Due to the interaction of the dislocation stress fields, approximately 50% of all dislocations are located close to the boundaries in the converged state and an internal structure can be observed.
In order to systematically analyze the impact of the number of dislocations (which is equivalent to the change of the initial dislocation density from a continuum point of view) on the dislocation structure in the system and the impact of the number of simulations on the ensemble averaging, we repeat the computations for different numbers of dislocations in the system while keeping the product of the number of dislocations n and the number of simulations m constant as $n \cdot m = 20000$. The ensemble averages of the discrete simulations for $n = 25, 100, 400, 800$ are shown in Fig.3. Due to the symmetry, only a quarter of the different configurations are shown. The results are

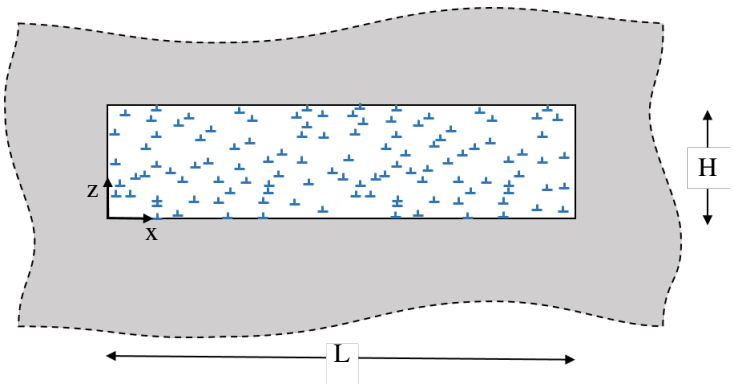

Figure 1: Bounded slip channel embedded into infinite elastic medium

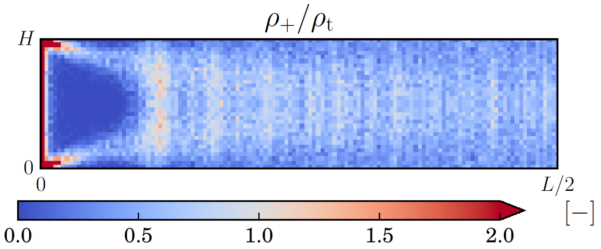

Figure 2: Ensemble average of the 1-Particle density of the slip channel with n=400 positive edge dislocations over m=200 discrete simulations. Due to the symmetry, only half of the system is shown.

symmetrized again along the x- and z-axis and normalized with respect to the average total dislocation density. The results show the change in the structural formation in the dislocation microstructure due to the impact of the boundaries. The finite slip system induces a dislocation free region close to the boundary which is increasing with increasing numbers of dislocations in the system. Also the structure observable inside the channel becomes more pronounced for larger numbers of dislocations.
In the following, we analyze the structure formation in the inner part of the system by considering the relative correlation function d_{++} according to equation (8) for the systems of $n = 25$ and $n = 800$ dislocations, see Fig. 4. Since the calculation of the correlation function requires a sufficiently homogeneous distribution of dislocations, just the inner 80% of the channel are considered by the effective measures ($\Omega_{\text{eff}} = [L_{\text{eff}} \times H_{\text{eff}}] = [0.1L, 0.9L] \times [0.1H, 0.9H]$). This also yields a reduced average number of dislocations n_{eff}. Here, the correlation function is computed considering the radius $0 \leq r \leq 3.5$ normalized by H_{eff}. The average dislocation spacing for each structure is depicted by a circular line. The results show a structure formation for both considered configurations, which is especially interesting since the structure formation for low numbers of dislocations was not visible in the 1-particle density in Fig. 3.
Based on these findings, we compare the configurations of $n = 25$ and $n = 800$ dislocations by applying the projection of the correlation function in x-direction which is derived by integration in y-direction $d^p_{++}(x)$ as

$$d^p_{++}(x) = \frac{1}{y_0} \int_0^{y_0} d_{++}(\mathbf{r}(x, y)\text{dy}. \tag{14}$$

Here, $y_0 = 0.25 H_{\text{eff}}$ is chosen. The results are shown in Fig. 5(left). An evaluation of the Fourier transform of $d^p_{++}(x)$ in the range of $[1.5H_{\text{eff}}, 3.0H_{\text{eff}}]$, see Fig. 5(right), shows a similar signature for both systems with a maximal amplitude $\Delta d^p_{++}(x)$ at a wave length $\lambda_{\text{struct}} = 0.374 H_{\text{eff}}$ independent of the number of dislocations. For the system with $n_{\text{eff}} = 9$, a large amplitude is also observed for a wave length around $\lambda = H_{\text{eff}}$.

4 Constitutive Modeling in the Discrete-continuum Transition

The analysis of the dislocation correlation function shows that a structure formation induced by the bounds of the system is not limited to a small region at the boundary but is also observed in the inner part of the system. Internal dislocation structures are already present for low numbers of dislocations in the system and become more pronounced at the boundary with an increasing dislocation content. Thus, it has to be investigated whether a

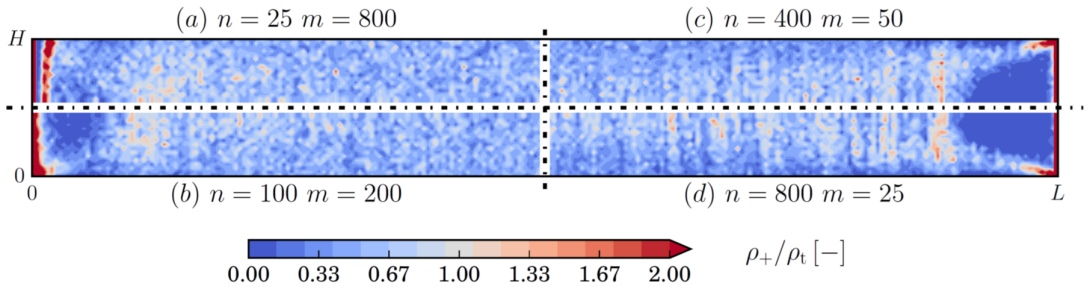

Figure 3: Ensemble average of the 1-particle density for a varying number of dislocations and varying number of simulations. The product $n \cdot m = const.$ for all representations. Due the symmetry of the system, just a quarter of each configuration is shown.

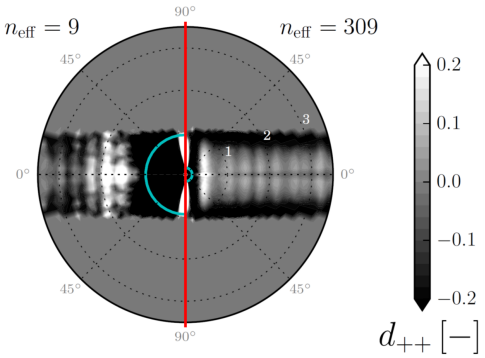

Figure 4: Comparison of the 2-particle-correlation functions d_{++} for the systems of $n = 25$ and $n = 800$ dislocations marked by the effective number of dislocations n_{eff}. The average dislocation spacing is denoted by the light half circles in the two systems, respectively. Due to the symmetry, just half of each system is shown.

homogenized continuum model in the discrete-continuum transition regime shows the ability to represent the characteristic internal dislocation microstructure of a bounded system.
We compare two approaches to incorporate dislocation short range interaction in the continuum constitutive formulations according to equation (11) and (12), which is considered in the dislocation based continuum model given by the evolution equations defined in (9 ,10). Here, the backstress parameter needed for τ_b is chosen as $D = 0.8$. We use the ensemble averages of the discrete dislocation dynamics results for $n \cdot m = 20000$ simulations as input configuration to the constitutive formulations and compute the residual fluxes f_{residuum} of the continuum representations given as

$$f_{\text{residuum}}(\rho_+, \tau_{\text{local}}) = \frac{\rho_+}{\rho_t} \frac{\tau_{\text{es}}(\rho_+) + \tau_{\text{local}}(\rho_+)}{\max|\tau_{\text{es}}(\rho_t)|}. \tag{15}$$

τ_{lokal} denotes herein τ_{nfc} or τ_b according to equation (11) and (12), respectively. The comparison of the residual fluxes for different discretization sizes of the discrete as well as the continuum system is given in Fig. 6 for $n = 400$ dislocations. The resolution is defined by $h_k = 2^{-k}H$. The results show the different ability of the continuum approaches to resolve the characteristic internal structure formation. For low resolutions, both models show similar results with moderate residual fluxes. Here, the main issue is the reproduction of the dislocation free zone behind a dislocation pile-up close to the boundary. Low residual fluxes are observed in the inner part of the system. However, the discretization of the system - in DDD as well as in the continuum - by just four elements over the height does not allow for the resolution of the internal structural details, since the edge length of an averaging volume is approximately the same as the internal structural length. For higher resolution the internal structures are more and more pronounced in the discrete data, which is captured by the approach using τ_{nfc} resulting in a homogeneous residual flux. With the approach using τ_{b} the residual flux fluctuates as the resolution increases. Further comparisons of the residual fluxes for different amounts of dislocations in the system ($n = 25$ and $n = 400$) are given in the Appendix. However, we want to remark, that the applied backstress model of Groma et al. (2003) is derived by the consideration of correlation functions for $\kappa/\rho << 1$. Here, the results show that the model yields good results if the general density in an averaging element is high enough. An extension of the model to $\kappa/\rho = 1$ by the consideration of the approach proposed in Groma et al. (2015) including a surface energy based boundary representation is an outstanding task.

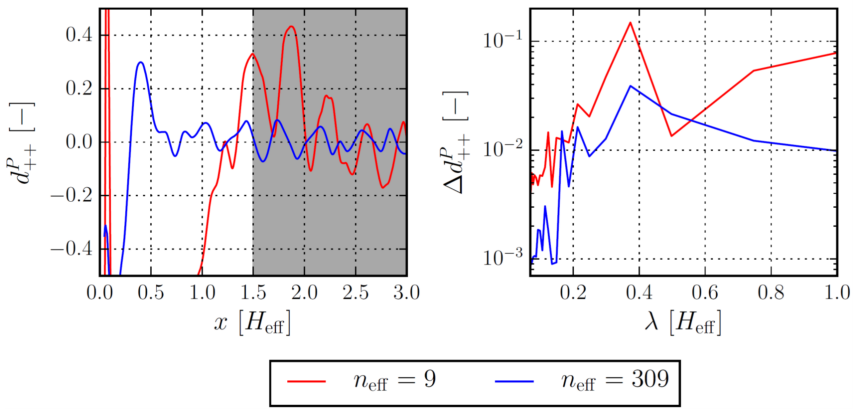

Figure 5: Projected correlation function d^p_{++} of the 2-particle density (left) and the corresponding Fourier transform in the range of $[1.5H_{\text{eff}}, 3.0H_{\text{eff}}]$ (right).

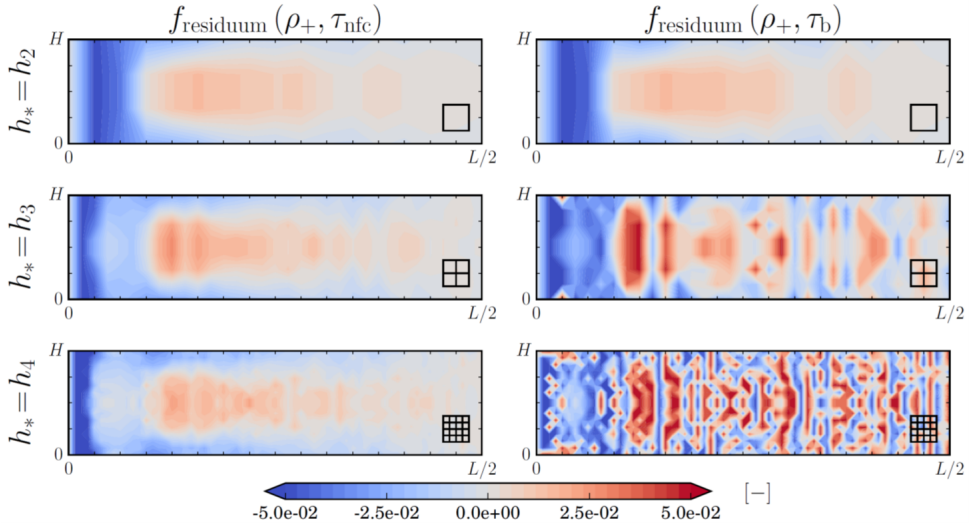

Figure 6: Comparison of the residual flux for different constitutive laws of dislocation interaction with respect to the ensemble average of n=100 dislocations for three different spacial discretization (depicted in the lower right edge of each figure).

5 Conclusion

A large number of 2d discrete dislocation dynamics simulations has been evaluated in order to compare ensemble averages for a varying number of dislocations and a varying number of simulations. A Fourier analysis was used to characterize the structural influence due to the strong dislocation walls at the boundaries. While the structural wave length $\lambda_{\text{struct}} = 0.374\mu$m can be observed macroscopically for $n = 800$ dislocations, it was surprising to also find it in the correlation function of $n = 25$ dislocations. Discussing the question, what features define a continuum limit for the transition regime from a discrete to a continuum model, it has been shown, that the internal length scale governed by the number of dislocations competes against the structural length scale of the system. In situations where the internal length scale is small compared to the structural length scale, the continuum models can be applied without special treatment of the boundary conditions. In situations where the internal length scale dominates the system (n small) a model as e.g. proposed in Groma et al. (2015) is needed to capture the dominating influence of the dislocation-dislocation correlation functions. The results show, that the impact of structural boundaries can not be reduced to a small boundary layer, but rather has a significant influence on the dislocation microstructure of the entire system. A comparison of the DDD data with a continuum formulation incorporating two variants for the modeling of homogenized dislocation stress fields demonstrates that the continuum approaches proposed in Schmitt et al. (2015) is a generalization of the continuum formulation of Groma et al. (2003), since it is able to represent the averaged dislocation system of GND densities also for $\rho \to 0$.Furthermore, it can be concluded, that the knowledge about the characteristic length scales of the internal

structure can be assumed to be a precondition to be able to conduct reliable continuum simulations with adequate spatial resolution.

6 Acknowledgments

The funding of this work by the European Social Fund and the state Baden-Wuerttemberg is gratefully acknowledged.

References

Acharya, A.: A model of crystal plasticity based on the theory of continuously distributed dislocations. *J. Mech. and Phys. Solids*, 49, (2001), 761–784.

Cleveringa, H. H. M.; VanderGiessen, E.; Needleman, A.: Comparison of discrete dislocation and continuum plasticity predictions for a composite material. *Acta Mater.*, 45, 8, (1997), 3163 – 3179.

Devincre, B.; Gatti, R.: Physically justified models for crystal plasticity developed with dislocation dynamics simulations. *AerospaceLab*, , 9, (2015), p–1.

Devincre, B.; Hoc, T.; Kubin, L.: Dislocation mean free paths and strain hardening of crystals. *Science*, 320, 5884, (2008), 1745–1748.

Dickel, D.; Schulz, K.; Schmitt, S.; Gumbsch, P.: A continuum formulation of stress correlations of dislocations in two dimensions. *Tech Mech*, 34, 3-4, (2014a), 205–212.

Dickel, D.; Schulz, K.; Schmitt, S.; Gumbsch, P.: Dipole formation and yielding in a two-dimensional continuum dislocation model. *Physical Review B*, 90, 9, (2014b), 094118.

El-Azab, A.: Statistical mechanics treatment of the evolution of dislocation distributions in single crystals. *Phys. Rev. B*, 61, (2000), 11956 – 11966.

Fivel, M.; Verdier, M.; Ganova, G.: 3d simulation of a nanoindentation test at a mesoscopic scale. 234, (1997), 923–926.

Franciosi, P.; Zaoui, A.: Multislip in fcc crystals a theoretical approach compared with experimental data. *Acta Metallurgica*, 30, 8, (1982), 1627–1637.

Groma, I.: Link between the microscopic and mesoscopic length-scale description of the collective behavior of dislocations. *Phys. Rev. B*, 56, (1997), 5807–5813.

Groma, I.; Csikor, F.; Zaiser, M.: Spatial correlations and higher-order gradient terms in a continuum description of dislocation dynamics. *Acta Mater.*, 51, (2003), 1271–1281.

Groma, I.; Vandrus, Z.; Ispánovity, P. D.: Scale-free phase field theory of dislocations. *Physical review letters*, 114, 1, (2015), 015503.

Hirth, J.; Lothe, J.: *Theory of dislocations*. Wiley, New York (1982).

Hochrainer, T.: Thermodynamically consistent continuum dislocation dynamics. *Journal of the Mechanics and Physics of Solids*, 88, (2016), 12–22.

Hochrainer, T.; Sandfeld, S.; Zaiser, M.; Gumbsch, P.: Continuum dislocation dynamics: towards a physical theory of crystal plasticity. *Journal of the Mechanics and Physics of Solids*, 63, (2014), 167–178.

Ispanovity, P. D.; Groma, I.; Gyorgyi, G.: Evolution of the correlation functions in two-dimensional dislocation systems. *Phys Rev B*, 78, 2, (2008), 024119.

Kubin, L.; Canova, G.: The modeling of dislocation patterns. *Scripta Metallurgica et Materialia*, 27, (1992), 957–962.

Reuber, C.; Eisenlohr, P.; Roters, F.; Raabe, D.: Dislocation density distribution around an indent in single-crystalline nickel: Comparing nonlocal crystal plasticity finite-element predictions with experiments. *Acta Materialia*, 71, (2014), 333–348.

Schmitt, S.; Gumbsch, P.; Schulz, K.: Internal stresses in a homogenized representation of dislocation microstructures. *Journal of the Mechanics and Physics of Solids*, 84, (2015), 528–544.

Schulz, K.; Dickel, D.; Schmitt, S.; Sandfeld, S.; Weygand, D.; Gumbsch, P.: Analysis of dislocation pileups using a dislocation based continuum theory. *Modelling Simul. Mater. Sci. Eng.*, 22, 2, (2014), 025008.

Schulz, K.; Sudmanns, M.; Gumbsch, P.: Dislocation-density based description of the deformation of a composite material. *Modelling and Simulation in Materials Science and Engineering*.

Sedláček, R.; Kratochvíl, J.; Werner, E.: The importance of being curved: bowing dislocations in a continuum description. *Phil. Mag.*, 83, (2003), 3735–3752.

Weygand, D.; Friedman, L. H.; van der Giessen, E.; Needleman, A.: Aspects of boundary-value problem solutions with three-dimensional dislocation dynamics. *Modelling Simul Mater Sci Eng*, 10, (2002), 437–468.

Zaiser, M.: Local density approximation for the energy functional of three-dimensional dislocation systems. *Physical Review B*, 92, 17, (2015), 174120.

Zaiser, M.; Miguel, M.-C.; Groma, I.: Statistical dynamics of dislocation systems: The inuence of dislocation-dislocation correlations. *Phys. Rev. B*, 64, (2001), 224102.

Zhu, Y.; Xiang, Y.; Schulz, K.: The role of dislocation pile-up in flow stress determination and strain hardening. *Scripta Materialia*, 116, (2016), 53–56.

A Appendix

The comparison of the residual fluxes of the continuum model with respect to the ensemble averages of the converged DDD configurations for different discretization sizes is given in Fig. 7 and Fig. 8 for $n = 400$ and $n = 25$ dislocations, respectively.

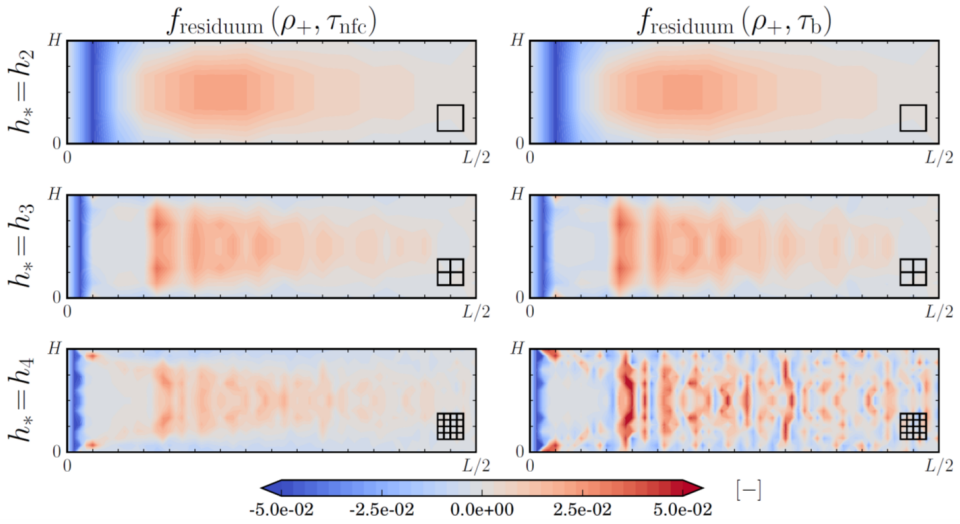

Figure 7: As Fig. 6 but with n=400 dislocation

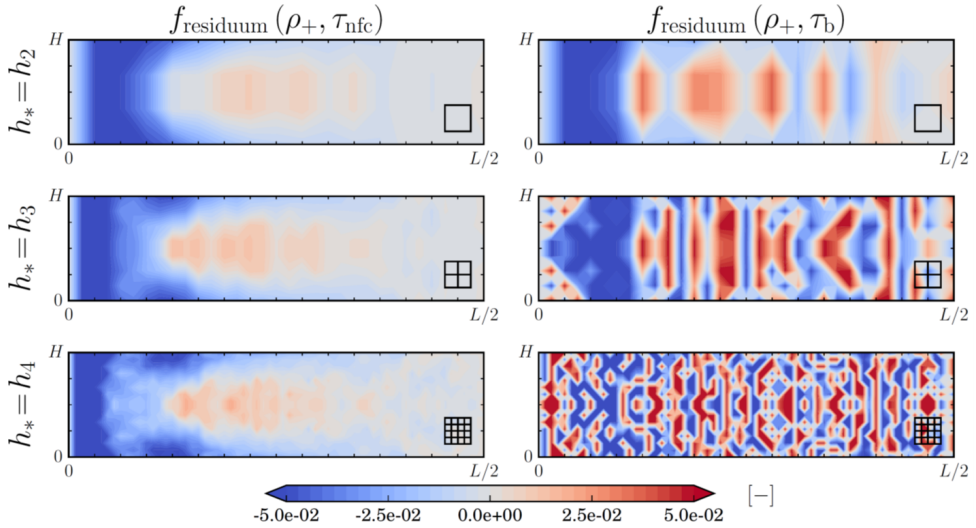

Figure 8: As Fig. 6 but with n=25 dislocation

Address: Institute of Applied Materials - Computational Materials Science
Karlsruhe Institute of Technology (KIT)
Kaiserstr. 12, 76131 Karlsruhe, Germany
email: katrin.schulz@kit.de